Corrosion resistance of CrN/NbN superlattice coatings grown by various physical vapour deposition techniques

HOVSEPIAN, P. E. <http://orcid.org/0000-0002-1047-0407>, LEWIS, D. B., LUO, Q. <http://orcid.org/0000-0003-4102-2129> and FARINOTTI, A.

Published version

HOVSEPIAN, P. E., LEWIS, D. B., LUO, Q. and FARINOTTI, A. (2005). Corrosion resistance of CrN/NbN superlattice coatings grown by various physical vapour deposition techniques. Thin Solid Films, 488 (1-2), 1-8.

Corrosion resistance of CrN/NbN superlattice coatings grown by various physical vapour deposition techniques

P. Eh. Hovsepian, D.B. Lewis, Q. Luo, A. Farinotti[1]

Sheffield Hallam University, Materials Research Institute, Howard Street, Sheffield, S1 1WB, UK
[1] LAFER S.p.A., Str. Di Cortemaggiore, 29010 Piacenza, Italy

Abstract: The corrosion and tribological performance of CrN/NbN superlattice coatings deposited by the techniques of unbalanced magnetron (UBM) sputtering, steered cathodic arc evaporation, and the combined steered cathodic arc and UBM sputtering, i.e. arc-bond sputtering (ABS), have been studied. In corrosion tests, the coatings grown by the ABS technique were superior to those grown by either UBM sputtering or arc evaporation with clear passivation behaviour and low corrosion current densities of 10^{-8} A·cm^{-2}. In tribological tests, the lowest coefficient of friction l =0.3 was shown by the arc evaporated coating whereas the CrN/NbN deposited by the ABS technique achieved the lowest dry sliding wear coefficient of Kc=5.0×10^{-15} m3·N^{-1}·m^{-1}. The microstructure of the coatings was investigated by cross-sectional transmission electron microscopy, X-ray diffractometry and energy dispersive X-ray spectroscopy, and was related to the corrosion and the tribological behaviour.

1. Introduction

In the recent years, the demand for novel and environmentally friendly technologies for corrosion and wear resistance coating deposition shows a tendency of constant increase. This tendency is particularly true in the case of the electroplated hard chrome, a coating with a long history of service in the industry. Owing to the relatively high values of hardness in the range of HV 10 GPa as a metal coating and the peculiar micro-cracked structure, hard chrome combines high corrosion with remarkable wear resistance. Environmental pressures, however, have initiated a worldwide research for its replacement. As an alternative, a superlattice structured CrN/NbN coating has been developed [1], employing the combined cathodic arc/unbalanced magnetron (UBM) sputtering deposition technique, i.e. arc-bond sputtering (ABS) [2]. Utilising the advantages of the nanoscale multilayers, hardness values approaching half the value of diamond have been achieved, combined with excellent corrosion behaviour due to the presence of the highly electrochemically stable niobium as a partner material [3,4]. Structural considerations, mainly porosity, have restricted the use of coatings grown by physical vapour deposition (PVD) for corrosion applications. It has been shown, however, that this potential danger can be overcome to a great extent by the superlattice approach [5] and careful engineering of the coating substrate interface [6], the bulk, as well as the surface of the coating [3]. The deposition technique strongly influences the quality of these important coating zones. It has been demonstrated that chemically modified interfaces can be developed if the sample surface is implanted by metal ions extracted from the arc discharge plasma, which leads to exceptionally high adhesion [7–9].Arc discharges would have been an ideal tool for deposition of pore-free coatings due to availability of highly energetic and mobile metal atoms and ions. However, the presence of the macroparticles (metallic droplets) generated from the cathode spots reduces the coating density and increases surface roughness. In contrast, magnetron sputtering provides smooth coatings, but they are often voided and porous, due to insufficient metal ionisation, which is detrimental to the corrosion and the wear resistance of these coatings. The aim of this work is to compare the corrosion and tribological performance of CrN/NbN superlattice coating deposited

by three commercially available deposition techniques, mainly arc evaporation, UBM sputtering and the ABS technique.

2. CrN/NbN superlattice coating deposition by various techniques.

2.1. CrN/NbN superlattice coating deposition by ABS

The ABS technique utilises metal ion etching for interface engineering and unbalanced magnetron sputtering for deposition of smooth macroparticle-free coatings [2,10]. CrN/NbN superlattice coatings have been deposited in industrially sized ¨1 m3, Hauzer HTC 1000-4 ABS vacuum coater [2]. The system comprises of four linear dual purpose (arc and UBM modes) plasma sources, surrounding a turntable, which provides three fold planetary rotations of the substrates. Fig. 1 outlines a schematic cross section of the machine, showing the target arrangement. The main technological

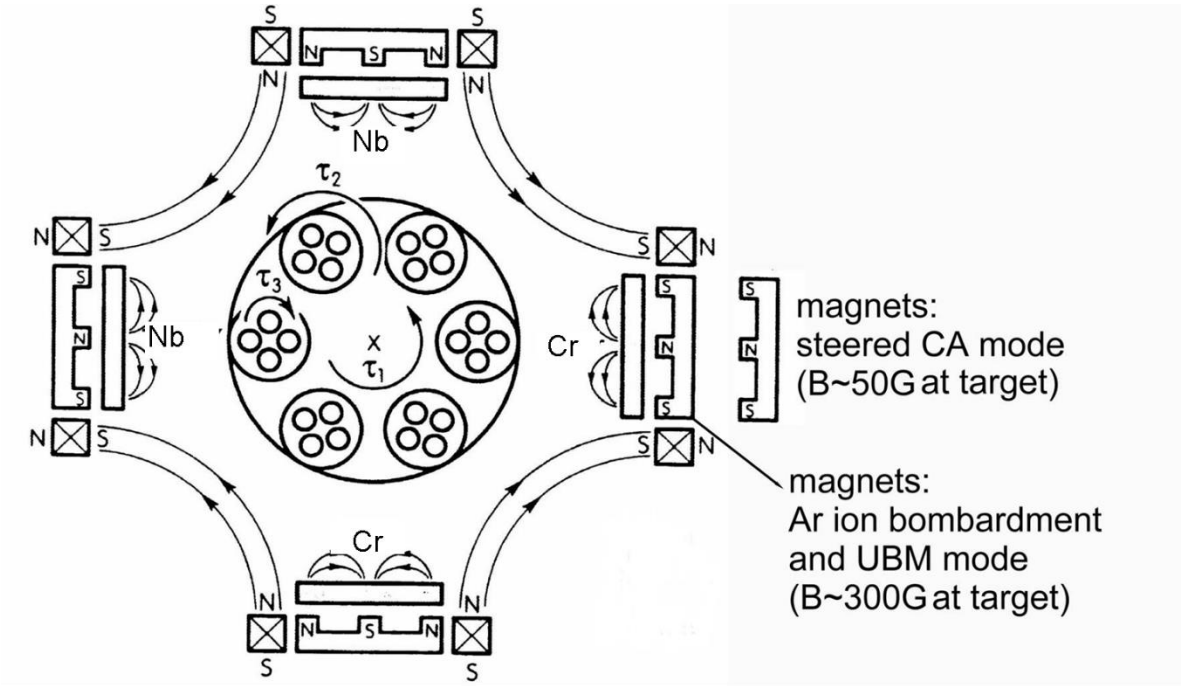

Figure 1 Schematic cross section of Hauzer HTC -1000 ABS coater.

steps as well as some deposition parameters are summarised in Table 1. During the ion-etching step, the substrate is bombarded with Cr+ ions accelerated to energies in the range of 2.5 keV, which produces intensive sputter cleaning and low energy metal ion implantation in the substrate material. The ions are extracted from a steered cathodic arc discharge sustained on one Cr target. Scanning

Table 1 Target and substrate bias voltage (Ub) selection for various superlattice coatings

PVD process	Target Configuration	Surface Pre-treatment	Base Layer	Superlattice Coating
UBM	Two Cr two Nb	Ar Ion Etch Ub = -1200V	CrN Ub = -75 V	CrN/NbN Ub = -120V
ARC	Two Cr one Nb arc sources	Cr Metal Ion Etch Ub = -1000V	CrN Ub = -100V	CrN/NbN Ub = -100V
ABS	Two Cr two Nb	Cr Metal Ion Etch Ub = -1200V	CrN Ub = -75 V	CrN/NbN Ub = -120V

transmission electron microscopy and energy dispersive Xray spectroscopy (STEM-EDXS) analysis revealed that 20 nm thick Cr implanted and structurally modified zone is formed, which promotes local epitaxial growth of the deposited coatings resulting in excellent adhesion to the substrate [8,9]. During this step, however, the surface is contaminated with macroparticles originating from the cathode spots of the arc discharge, which become in later stages sources for growth defects and coating porosity [8,11]. Following the ion-etching step, a 0.3 Am thick single phase CrN base layer is deposited to provide smooth transition in hardness and stress between the substrate and the CrN/NbN coating. The CrN/NbN superlattice coating is produced by sequential exposure of the coated surfaces to the four unbalanced magnetrons furnished with Cr and Nb targets. The precision of the superlattice periodicity is controlled by the power dissipated on the targets, the partial pressure of the reactive gas, the bias voltage applied to the substrate and the primary rotation speed of the turntable.

2.2 CrN/NbN superlattice coating deposition by UBM sputtering

To eliminate the negative effect of the macroparticles on the coating's porosity and corrosion resistance, the metal ion-etching step of the ABS technology was replaced by Ar^+ ion etching. The argon plasma was generated by operating one magnetron furnished with a Cr target at very low power of 0.5 kV to avoid deposition of Cr on the substrate surface. A high substrate bias voltage

(Ub) of -1200 V was applied in the ion-etching stage to make effective cleaning. The CrN base layer and CrN/NbN superlattice coating were then deposited on droplet-free surface by unbalanced magnetron sputtering. In these trials, the same equipment and similar technological parameters as for the ABS coatings have been used in order to minimise as much as possible the differences between the two coatings (see Table 1).

2.3 CrN/NbN superlattice coating deposition by cathodic arc evaporation

Although arc coatings suffer from the drawbacks of the droplet phase, utilising highly ionised, metal plasma for coating deposition has a great potential to produce fine structured films. Similar to the ABS technology Cr^+ ion etching was employed as surface pre treatment step, followed by deposition of CrN base layer and CrN/NbN superlattice coating, vaporised from a three linear steered cathodic arc sources in pure nitrogen atmosphere in a Hauzer HTC 1000-3 system, Table 1. CrN/NbN has been deposited on mirror polished samples from 316 stainless and M2 high speed steel, to carry out corrosion and tribological tests respectively. Prior to the coating deposition, the samples were cleaned in ten stages automatic cleaning line, containing a range of aqueous based alkali detergents and deionized water.

3. Characterisation techniques.

The microstructure and properties of the CrN/NbN superlattice coatings were characterised using various techniques.

Various X-ray diffraction (XRD) techniques based on a Philips PW 1710 automated diffractometer were applied using Ka-Cu (λ =0.15405 nm) to determine the crystalline structure, superlattice period and residual stress. The superlattice period D was quantified from patterns obtained from low angle (2θ =1° - 10°) and high angle (2θ =20° - 140°) scanning using the Bragg-Brentano geometry. The residual stress was determined by X-ray glancing angle diffractometer utilising the $\sin^2\psi$ method. More details of the XRD methods have been described elsewhere [1]. A transmission electron microscope (TEM, Philips CM20, 200 kV) was applied to characterise the interface and

cross-sectional microstructure of the coatings. The final stage of TEM sample preparation was performed on a Gatan-691 precision ion polishing system.

The coating surface roughness was measured using a mechanical stylus profilometer (Rank Taylor Hobson Talysurf). The hardness was measured using Knoop indentation (Mitutoyo MVK-G1) at an indenting load 0.025 kg. The coating scratch adhesion property, i.e. critical load Lc, was determined on a scratch tester (CSM REVETEST). A CSM pin-on-disc tribometer was used to evaluate the wear behaviour of the coatings at test conditions of: 6 mm in diameter Al_2O_3 balls, load 5 N, linear speed 0.1 $m \cdot s^{-1}$, sliding duration 60,000 laps (total sliding distance: 4.5 km).

Electrochemical corrosion evaluation of the coatings was carried out by potentiodynamic polarisation method on a Solartron Model 1286 potentiostat unit. Samples were polarised in 0.5 M NaCl solution with an exposed sample area of 1 cm^2 in 1-l electrochemical cell. The potential sweep rate was 0.02 $V \cdot min^{-1}$ with a standard calomel reference electrode. The solution was naturally aerated but otherwise not stirred during testing.

4. Results and discussion

4.1 Phase composition and texture of the various CrN/NbN superlattice coatings

Low angle XRD patterns from the CrN/NbN coatings deposited in cathodic arc, ABS and UBM modes are shown in Fig. 2a. The superlattice periods, Δ for the cathodic arc, ABS and UBM deposited coatings were 3.8 nm, 3.2 nm and 3.7 nm respectively, see Table 2. It is clear from the XRD patterns for the cathodic arc deposited coatings that second and third order reflections are appearing. This is in contrast to the two CrN/NbN coatings deposited by (ABS) and (UBM). These results clearly indicate that in arc deposited coatings the interfaces between the individual component layers of the film are obviously flatter and better defined than in those produced at similar bias voltages by ABS and UBM sputtering. Although the bias voltage of –100 V used when depositing cathodic arc coatings is slight lower than the bias voltage for the ABS and UBM

deposited coatings, namely –120 V in both cases. The increased ion-charge during arc deposition (Nb^+) compared with (Nb^+) for ABS and UBM

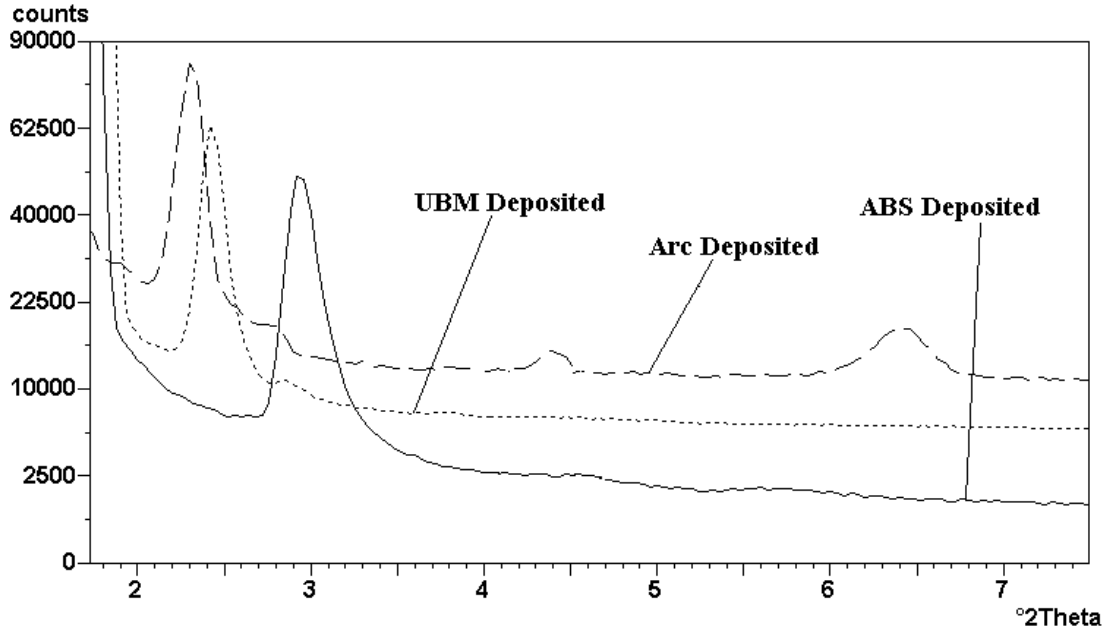

(a)

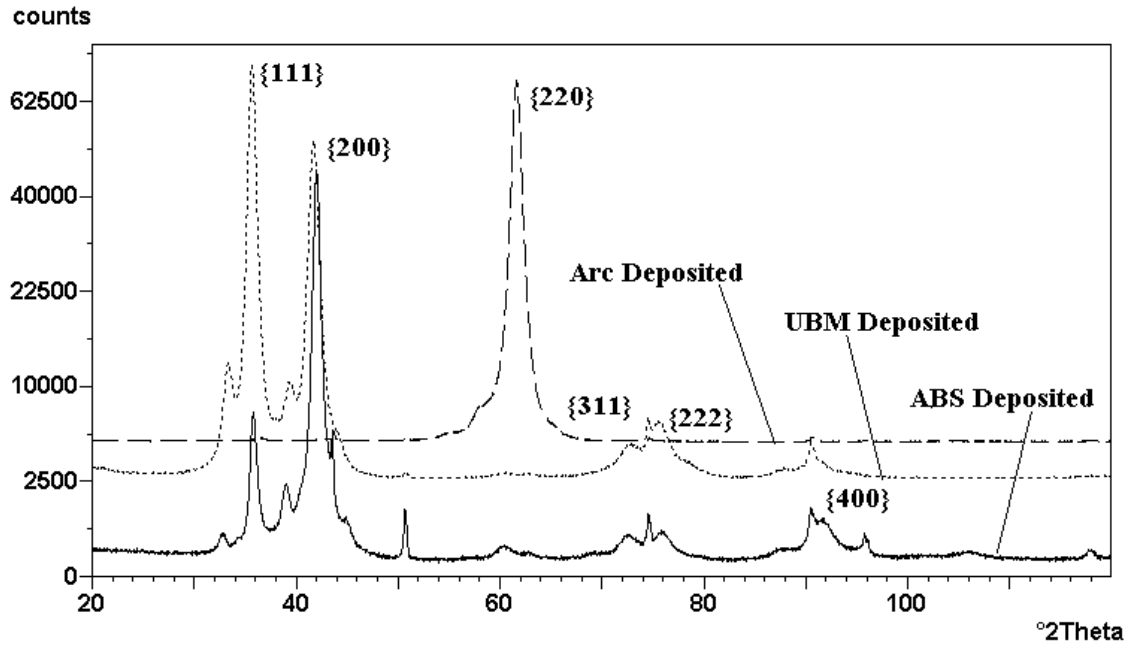

(b)

Figure 2 X-ray diffraction patterns from CrN/NbN superlattice coating deposited by various deposition techniques: a) low angle, b) high angle diffraction patterns.

deposition [12] results in an ion energy of 300 eV for the arc deposited coating compared with 120 eV for the ABS and UBM deposited coatings. This enhanced ion bombardment for cathodic arc

deposited films, results in an increased ad-atom mobility and re-sputtering which suppresses interface-roughening effects [8] and therefore produces the smoother interfaces.

Table 2 Superlattice period (Δ), thickness, surface roughness (Ra), mechanical and tribological properties, and texture factor of various coatings

Coating	Δ [nm]	Thickness [μm]	$HK_{0.25}$ [GPa]	Lc [N]	Stress [GPa]	Friction Coeff.	Wear Coeff. [10^{-15} m^3 $N^{-1}m^{-1}$]	Ra [μm]	Texture T* %
UBM CrN/NbN	3.7	4.5	33.3	18	- 6.3	0.95	9.2	0.036	$T^*_{\{111\}}$ =45.1%, $T^*_{\{100\}}$ =35.1 %
ARC CrN/NbN	3.8	5.8	35.3	46	- 6.83	0.3	6.2	0.09	$T^*_{\{110\}}$ = 97.5 %
ABS CrN/NbN	3.2	4.5	36.3	62	- 6.5	0.9	5.0	0.033	$T^*_{\{100\}}$ = 77.4 %
Hard Cr	NA	25	14.2	15	-1.6	0.72	58	0.05	$T^*_{\{111\}}$ = 98.8 %

High angle XRD for the cathodic arc, ABS and UBM deposited CrN/NbN coatings are shown in Fig. 2b. The structures were found to be all single-phase fcc structures (NaCl) and it was not possible to resolve individual reflections from the CrN and NbN phases. The peak positions represent the weighted-mean of the individual reflections from the CrN and NbN phases [13]. The XRD patterns show intense {200} and {220} reflections for the ABS and arc deposited coatings respectively. In contrast in the UBM film the {111} and {200} reflections were of almost equal intensity. Quantitative textural measurements based on the XRD data using the Harris [14] inverse pole figure method, are included in Table 2. The arc deposited CrN/NbN superlattice film exhibited an extremely strong {110} texture (T* =97.5 %) which is in contrast to ABS deposited CrN/NbN superlattice which exhibited a pronounced {100} texture (T* = 77.4 %). The UBM deposited film exhibited a mixed {111} (T* = 45.1 % and {100} (T* = 35.1 %) texture. Pronounced {110} textures are observed in arc deposited CrN coatings when bias voltages of –50 V and above are used during the deposition process [15,16]. The pronounced {100} texture observed in the ABS deposited film is consistent with previous work on CrN/NbN ABS deposited films (at bias voltages between –75 V and –120V)[17].

Residual stress measurements for and cathodic arc, ABS and UBM deposited CrN/NbN coatings are included in Table 2. All coatings exhibited similar residual compressive stress states with values in the range 6.3 to 6.8 GPa with the arc deposited coating having the highest residual stress. These high residual stresses clearly reflect the high bias voltages ($U_B \geq -100$ V) used during deposition of all three coatings. In a similar manner to those observed in monolithically grown coatings increases in stress can be attributed to the formation of defects by energetic ion bombardment during deposition [18].

4.2 XTEM characterisation of the ABS, UBM and Arc CrN/NbN superlattice coatings

TEM analyses were carried out to reveal the main structural differences resulting from the different conditions for CrN/NbN superlattice coating growth, provided by the UBM, ABS and Arc methods. Previous research has shown that the bombarding species, Ar^+ or metal ions, used for surface pre-treatment can, dramatically influence the microchemistry and structure of the interface region [7, 10]. Fig.3 a,b,c show the structure of the interface region and the adjacent CrN base layer of various CrN/NbN superlattice coatings deposited on stainless steel substrates. Etching with accelerated Ar^+ ions often fails to remove completely the existing surface oxide layers and leads to entrapment of large amounts of gas phase resulting in formation of Ar bubbles [6, 7]. These lower mass density regions can be observed as a fine-grained ribbon built over the substrate surface and buried under the CrN base layer, Fig.3a. In contrast the structure of the Cr^+ metal ion etched interface shows features, which are typical for the ion- implanted surfaces. The irradiation of the steel surface with metal ions causes substrate grain refinement to a depth of 7-10 nm, Fig. 3 (b) and (c). STEM-EDX analyses have shown that the composition of this top region of the substrate is significantly modified, enriched in Cr up to ~ 30 at. % [6]. This extremely dense, metal ion implanted interface provides excellent adhesion and high barrier properties as a main advantage for both ABS and Arc deposited CrN/NbN coatings. Other interesting structural differences can be observed in the CrN base layer. The CrN base layer of both arc and UBM deposited CrN/NbN coatings show a distinct columnar morphology. In the case of the arc deposited coating this is highly dense and void- free,

Fig.3c. In contrast the base layer of the UBM deposited coatings is porous with intercolumnar voids initiated at very early stages of the coating growth. On the other hand, ABS coatings are much denser, showing ~ 100 nm

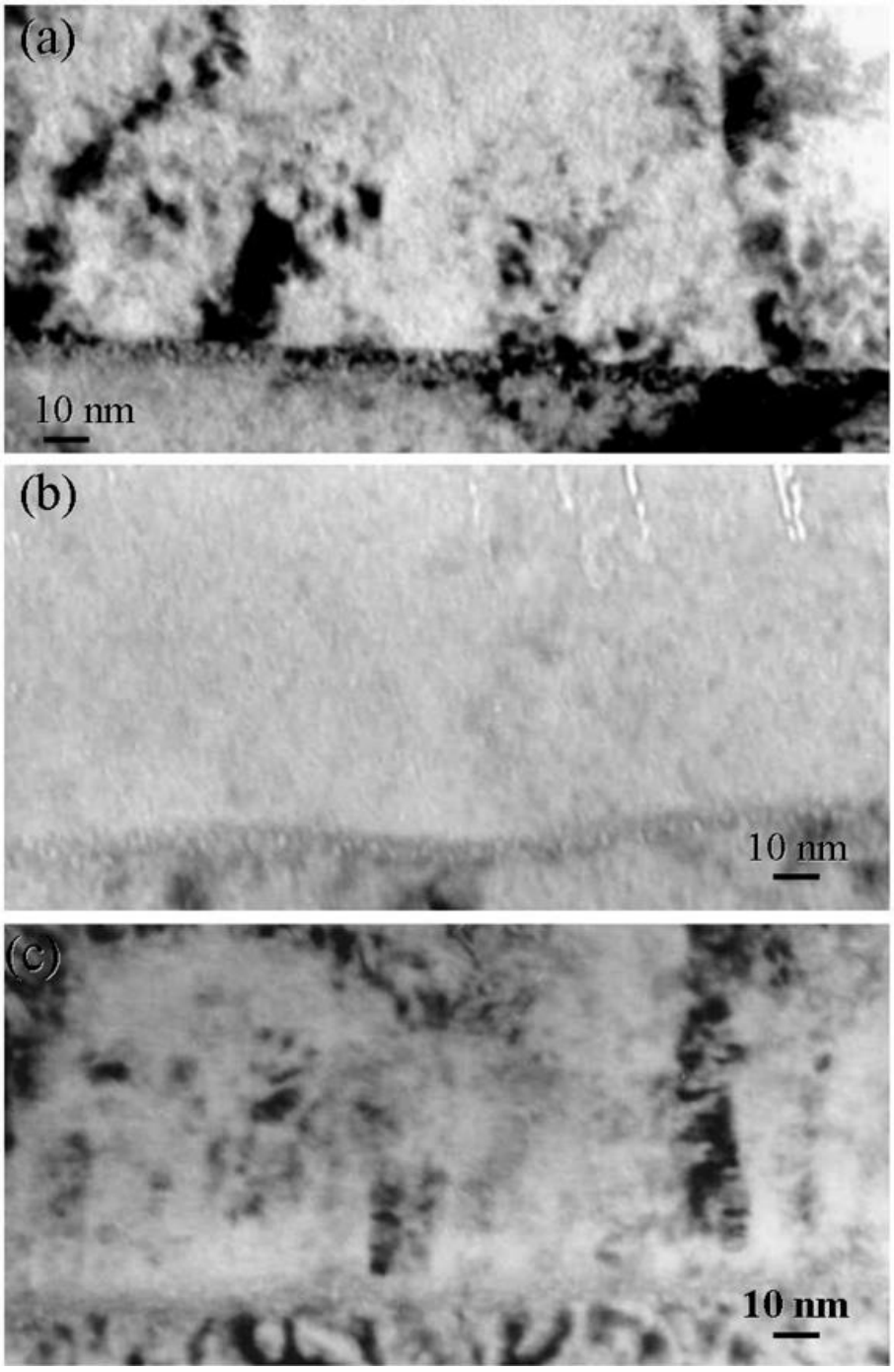

Figure 3 Bright field TEM image of the interface and CrN base layer of CrN/NbN deposited by different processes. (a) UBM-Ar etching; (b) ABS-Cr ion etching;(c) Arc-Cr ion etching.

thick void-free CrN region adjacent to the interface and a sub-dense region localised only on the top of the layer, Fig. 3b. Furthermore, in contrast to the UBM coating the dense ~ 100 nm thick base layer region in the ABS coating shows the same diffraction contrast indicating that the same crystallographic orientation extends over the entire region shown in Fig. 3b. Previous work [19]

has shown that this is indicative of local epitaxy between coating and substrate, which imparts excellent adhesion between coating and substrate. In both cases however, the voids developed in the CrN base

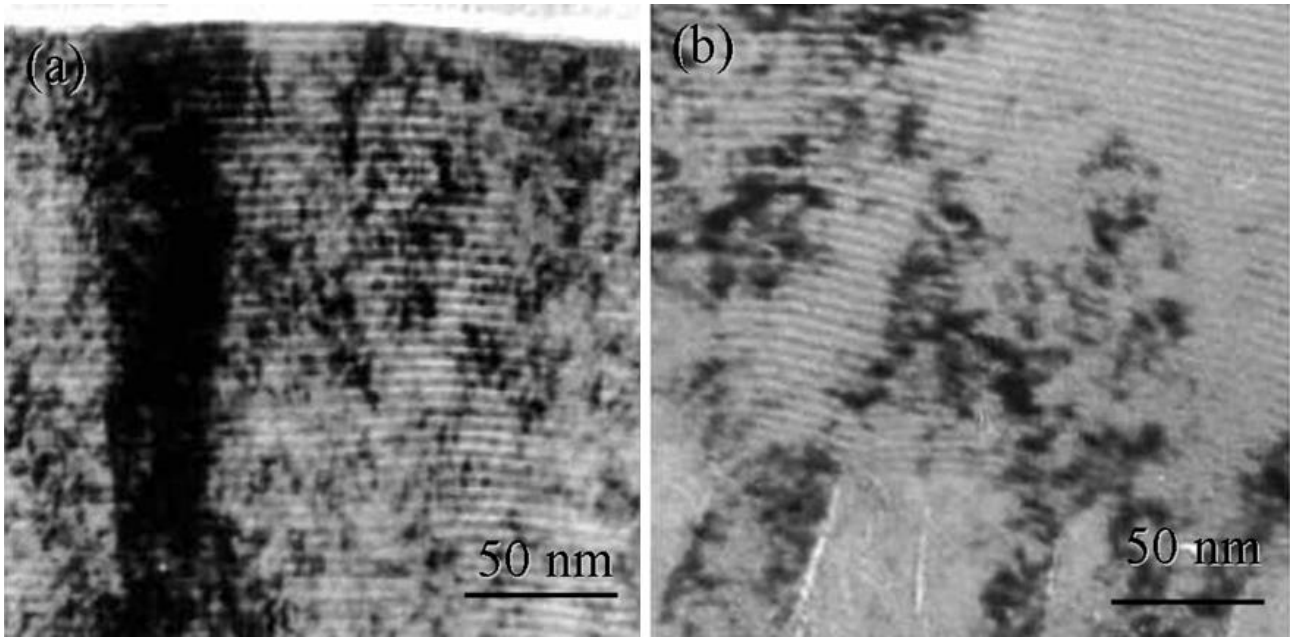

Figure 4 Bright field TEM image of the CrN/NbN superlattice coating deposited by ABS technique. (a) At base layer superlattice coating region; (b) At the top surface region of the coating.

layer do not propagate further in the superlattice structured CrN/NbN coating, Fig. 4b. All three coatings show very dense, and very precise nanoscale multilayer structure, with layers almost parallel to the substrate (low superlattice waviness), Fig. 4 a, b. This more perfected structure results from the intensive ion bombardment during growth (pre-selected higher bias voltage for the UBM and ABS, and high metal atoms ionisation in the Arc case), which causes higher ad atom mobility and re-sputtering of the weakly bonded atoms from the condensation surface. Fig 4a shows also that the top surface of the UBM and ABS CrN/NbN coatings is extremely smooth and almost free from growth defects. Fig. 5 shows the structure of Arc deposited CrN/NbN superlattice coating. The single phase columnar grown CrN base layer is followed by an extremely dense and fine structured CrN/NbN multilayer coating. The main disadvantage of the arc evaporation, the ejection of macroparticles or “droplets”, which generally deteriorates the density and the roughness of the coatings seems not to be as critical in coatings with superlattice structure. Quick self-healing of growth defects originating from droplets was observed to occur in the arc deposited CrN/NbN

coatings. It can be seen in Fig. 5, the magnified fragment, that the growth defect generated from a "droplet" annihilates after further deposition of approximately 70 nm (200 bilayers) thick superlattice coating on the top. Thus, the growth defects remain buried within the coating and do not reach the surface, which contributes to enhanced coating density. The observed self-healing effect could be attributed to the high compressive stress and increased ad-atom mobility in arc deposited coatings.

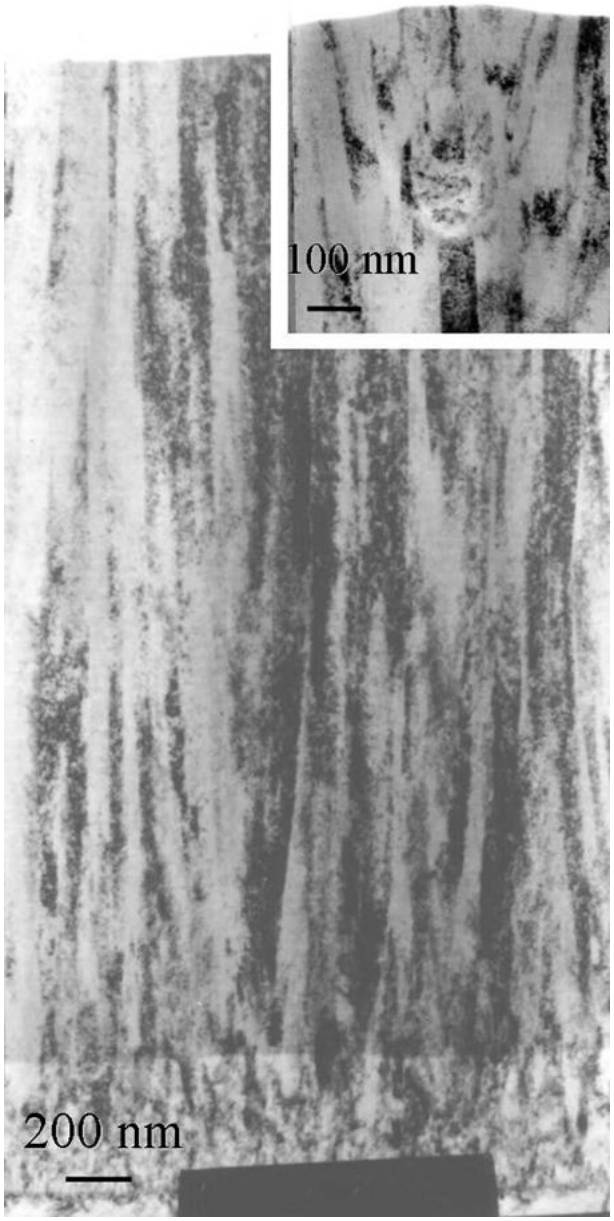

Figure 5 Bright field TEM image of CrN/NbN superlattice coating deposited by Arc evaporation technique. Magnified fragment-macroparticle (droplet) and the associated growth defect

4.3 Mechanical and tribological properties of the various CrN/NbN superlattice coatings.

Table 2 summarises the results from the mechanical and tribological tests of the CrN/NbN superlattice coatings deposited by ABS, UBM and Arc deposition techniques. The ABS and UBM

coatings were in a similar thickness range of 4.5µm, whilst Arc coatings were somewhat thicker in the 5.8µm range. Although the superlattice period for UBM and ABS CrN/NbN coatings was similar, the UBM coatings showed lower hardness values. Both UBM deposited coatings were smoother, Ra values in the range of 0.03µm, than Arc deposited coatings (Ra= 0.24µm), due to the well known effect of the droplet phase on this parameter. Arc and ABS coatings, which utilise metal ion etching as surface pre-treatment, showed higher scratch adhesion values of Lc= 46 N and Lc= 62 N respectively. Independent from the residual stress exceeding 6 GPa, the quality of the ion-implanted interface allows for tolerating higher stress, thus providing excellent adhesion and mechanical properties of the films. It has been demonstrated that in dry high speed milling operations, where the coating is exposed to high and very often impact mechanical load and thermal shocks the coating performance is directly related to its adhesion [10]. Not surprisingly, weaker coating-substrate bonding, (Lc= 18N) was achieved by the argon ion etching, which could be explained by the structure of the interface and CrN base layer (Fig. 3a). The accumulation of argon at the interface region, together with the voided structure of the following layer contributes to easier coating delamination under applied mechanical load [7, 9]. The tribological tests further magnified the inferior behaviour of the UBM coatings under high mechanical stress. Although fine multilayer structures show excellent wear behaviour, which is characterised by fine layer by layer material removal mechanism during sliding and are less prawn to plastic deformation [20], UBM deposited coatings showed the highest coefficient of friction and two the times wear coefficient when compared to the ABS coatings. The highly defected interface region and voided base layer obviously weaken the load bearing capacity leading to easy development of tensile cracks and premature delamination, which becomes detrimental to the coatings friction and wear performance. The lowest coefficient of friction of 0.3 was measured for the Arc deposited CrN/NbN superlattice coating. One possible reason for this unusual behaviour could be the very strong crystallographic texture of the coating. As 99.7 % of {110} planes are oriented parallel to the substrate (see Table 2), which during dry sliding provides conditions for a very fine nanoscale layer material removal

(shearing over individual atomic planes with similar orientation). The wear rate of the Arc CrN/NbN coatings however, is inferior to that of the ABS grown coatings, which is believed to be due to the presence of the soft macroparticles embedded in the coating. The ABS CrN/NbN coating on the other hand, combines the strong arc bonding to the substrate with a droplet free, therefore smooth superlattice structured bulk of the coating, resulting in higher wear resistance. Owing to their special structure and enhanced hardness, PVD CrN/NbN superlattice coatings show one a order of magnitude better wear coefficient compared to that of hard chrome, independent of the deposition method, (see Table 2).

4.4 Corrosion behaviour of the ABS, UBM and Arc CrN/NbN superlattice coatings

The corrosion resistance of the PVD coatings depends not only on the degree of porosity resulting mainly from the structural defects but also from factors, such as coating-substrate interface chemistry, structure [5], surface defect density [3], coating adhesion and stress levels [21]. Most of these parameters are intrinsically connected, therefore the best match of deposition conditions required to meet such complex inter relations, will strongly depend on the deposition method used for coating production. Potentiodynamic polarisation results shown in Fig. 6a indeed demonstrate the wide span in the corrosion behaviour of similarly superlattice structured CrN/NbN coatings deposited by the UBM, Arc and ABS techniques. The least corrosion resistance from the three coatings was provided

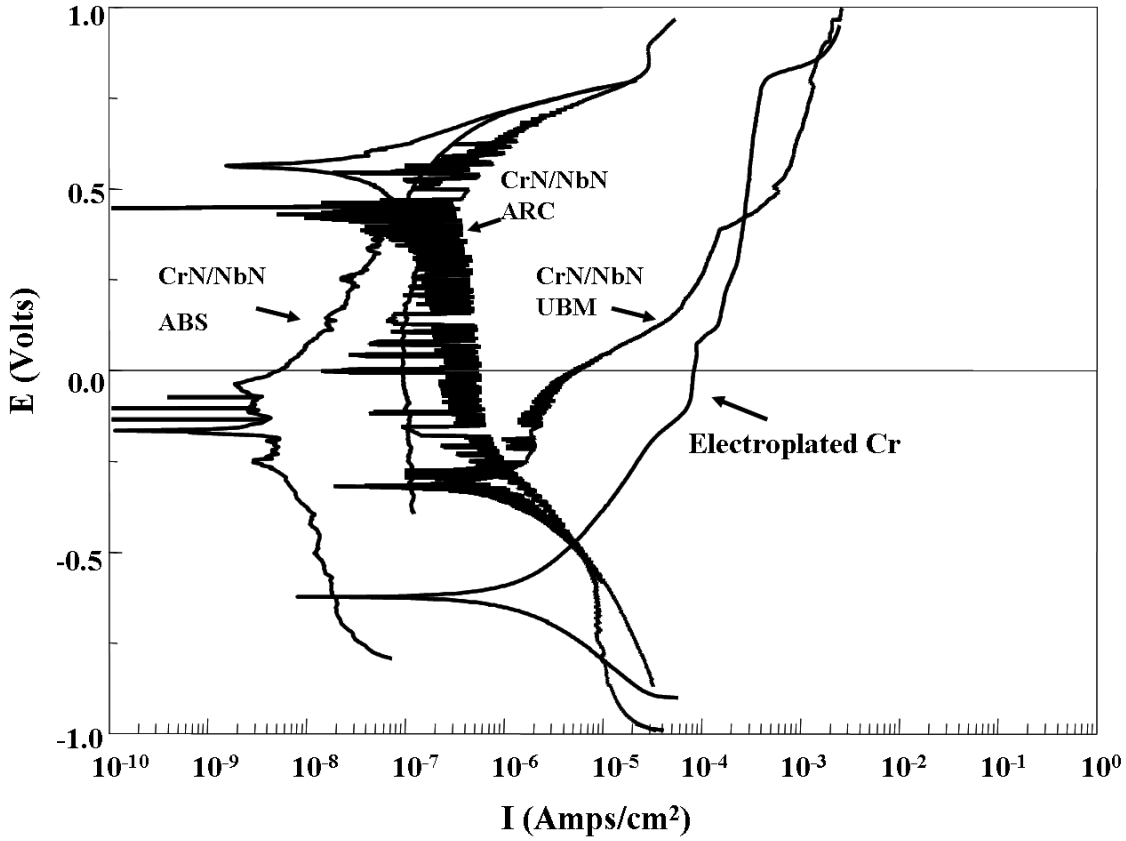

Figure 6 Potentiodynamic polarisation curves of CrN/NbN superlattice coatings taken in 3% Na Cl electrolyte. (a) Deposited by various PVD techniques; (b) Deposited by ABS technique utilising Nb^+ ion etching.

by the UBM coating, which utilises Ar^+ ion etching for substrate pre-cleaning. Previous work on PVD Nb coatings [4, 5] has shown the inferiority of the sub dense Ar^+ etched interface in corrosion applications. The corrosion resistance is further reduced by the presence intercolumnar voids in the CrN base layer (see Fig 3a). Only a narrow passivation shoulder, mainly in the region where the coating was cathodically polarised was observed with corrosion current densities in the range of 10^{-6} to 10^{-5} A. cm^{-2}. The corrosion current was steadily increasing, showing diffusion controlled pitting behaviour replaced by a clear pitting event at + 320mV. In contrast both, (ABS and Arc), CrN/NbN coatings, utilising metal ion treated interface, showed one to two orders of magnitude lower corrosion currents and much better passivation behaviour in comparison with the UBM coating. Surprisingly Arc deposited CrN/NbN demonstrated exceptionally dense structure from an electrochemical point of view, despite the large amount of droplets embedded in the coating. The very well known source for droplet related voids observed with monolithically grown coatings did

not operate in the case of the superlattice structures. The XTEM analysis indeed showed that a specific "self healing" effect takes place, which closes very effectively the growth defects originating from droplets in the nanoscale multilayers, (see Fig. 5). The higher ad- atom mobility due to the higher arriving energies of the atoms 200 eV and 300 eV for the Cr and the Nb respectively, combined with the hindered evolution of growth defects leads to significant densification of the Arc deposited coatings and therefore to excellent corrosion protection of the substrate material. In the conditions of this experiment, best results were achieved by the ABS deposited CrN/NbN superlattice coatings. Low corrosion current densities ranging between 10^{-8}-10^{-7} A.cm^{-2} were measured, and no coating pitting was detected as indicated by the reverse part of the polarisation curve (see Fig. 6a). The ABS CrN/NbN coatings corrosion resistance can be further enhanced by replacing the Cr^+ ion etch with Nb^+ ion etch, which decreases the corrosion current density into the 10^{-9}A.cm^{-2}- 10^{-8}A.cm^{-2} range, Fig. 6b. It has been shown previously [3, 6] that using Nb^+ as etching species dramatically alters the composition, structure and therefore the corrosion properties of the coating substrate interface. Along with the typical for the metal ion etching Nb implantation profile, an 8-10nm thick nanocrystalline, almost amorphous layer of Nb is deposited, which acts as a barrier to the corrosion solutions to reach the substrate. CrN/NbN coatings deposited at Ub= - 75V show a broad passivation shoulder in the polarisation curve with increased pitting potential up to +800mV, Fig. 6b. A complete suppression of the pitting events and exceptionally low, corrosion current densities in the range of 10^{-9} A. cm^{-2} can be achieved if the Nb^+ ion etching is combined with higher bias voltage (Ub = - 120V).to produce very smooth CrN/NbN coatings [3]. It has to be mentioned also that ABS and Arc CrN/NbN superlattice coatings, in the conditions of the potentiodynamic polarisation test, showed significantly higher corrosion protection than that of electroplated hard chrome. The special superlattice structure is seen as an advantage of these novel coatings to provide combined wear and corrosion protection, which has already been utilised in a number of successful industrial applications [22].

Conclusions

CrN/NbN superlattice structured PVD coatings have been developed combining high wear resistance with high corrosion resistance which are seen as very advantageous in niche applications where hard chrome has been successfully used so far. The protection capacity of these novel coatings depends on the deposition technique utilised for the production. Technologies employing metal ion etching/ implantation as a pre cleaning step (ABS and Arc) are superior to the ones based on Ar^+ ion etching (UBM) Owing to the smoother and with less amount of growth defects surface, ABS coating showed the best performance both in wear and corrosion tests. The ultimate corrosion performance has been achieved when Nb^+ ion etching was utilised prior to the deposition of CrN/NbN superlattice coatings by unbalanced magnetron sputtering.

Acknowledgements:

The development of CrN/NbN superlattice coating took place within the BRITE EURAM research project NEWCHROME, No BE-96-3305, the financial support of the EU as well as the intellectual support of all partners is gratefully acknowledged.

References

[1] P. Eh. Hovsepian, D.B. Lewis, W.-D. Münz, Surf. Coat. Technol. 133-134 (2000) 166.

[2] W.-D. Münz, D. Schulze and F. Hauzer, Surf. Coat. Technol. 50 (1992) 169.

[3] P. Eh. Hovsepian, D. B. Lewis, W.-D. Münz, Surf. Coat. Technol. 133-134 (2000) 166.

[4] H. Paritong, I. Wadsworth, L.A. Donohue, W.-D. Münz, Trans IMF 76 (1998) 144.

[5] M. Tomlinson, S. b. Lyon, P. Eh. Hovsepian, W.-D. Münz: Vacuum 53 (1999) 117.

[6] C. Schonjhn, H. Paritong, W.-D. Münz,, R.D. Twesten, I. Petrov: J. Vac. Sci. Technol. A19 (2001) 1392.

[7] G. Håkansson, L. Hultman, J.-E. Sundgren, J. E. Greene, W.-D. Münz, Surf. Coat. Technol., 48 (1991) 67.

[8] I.Petrov, P. Losbichler, D. Bergstrom, J.E. Greene, W.-D. Münz, T. Hurkmans and T.Trinh, Thin Solid Films 302 (1997) 179.

[9] C. Schönjahn, D.B.Lewis, W.-D. Münz, I. Petrov, Surf. Eng. 16 (2000) 176.

[10] W.-D. Münz , C. Schönjahn, H. Paritong, , I.J. Smith, Le VIDE, 3-4 (2000) 205.

[11] W.-D. Münz, I.J. Smith, D.B. Lewis, S. Creasey, Vacuum 48 (1997) 473.

[12] A. Anders, Phys. Rev. E55 (1997) 328.

[13] G. Håkansson, PhD. Dissertation, 255, Linköping University, Linköping, 1991

[14] G. B. Harris Phil. Mag. 43 (1952) 113.

[15] C. Gautier, H. Moussaoui, F. Elstner, J. Machet, Surf. Coat. Technol, 86-87 (1995) 254.

[16] T. Hurkmans, D. B. Lewis, H. Pariton, J.S. Brooks, W.-D. Münz, Surf. Coat. Technol. 114 (1999) 52.

[17] D. B. Lewis, P. Eh. Hovsepian, W.-D. Münz, 7th International Symposium on Trends and Applications of Thin Films, Société Français du Vide, March 2000, Nancy, France, P 20.

[18] I. Petrov, L. Hultman, U. Helmersson, J.-E. Sundgren, J. E. Greene, in PhD Thesis Lars Hultman, Linköping Studies in Science and Technology 186, 1988, Linköping University.

[19] C. Schönjahn, L. A. Donohue, D.B.Lewis, W.-D. Münz, R. D. Tweeston, I. Petrov, J. Vac. Sci. Technol. 18 (2000) 1718.

[20] Q.Luo, W.M. Rainforth, W.-D. Münz, Wear 225 (1999) 74.

[21] P.Eh. Hovsepian, D.B.Lewis, W.-D. Münz, S.B. Lyon, M. Tomlinson, Surf. Coat. Technol. 120-121 (1999) 535.

[22] W.-D. Münz, D.B.Lewis, P.Eh.Hovsepian, C. Schonjhn, A. Ehiasarian, I.J. Smith, Surf. Eng. 17 (2001) 15